Geophysical Research Letters

RESEARCH LETTER
10.1029/2023GL106456

Frequency Chirping of Electromagnetic Ion Cyclotron Waves in Earth's Magnetosphere

Zeyu An[1,2], Xin Tao[1,2], Fulvio Zonca[3,4], and Liu Chen[4,5]

[1]Deep Space Exploration Laboratory|Department of Geophysics and Planetary Sciences, University of Science and Technology of China, Hefei, China, [2]CAS Center for Excellence in Comparative Planetology|CAS Key Laboratory of Geospace Environment, Hefei, China, [3]Center for Nonlinear Plasma Science and C.R. ENEA Frascati, Frascati, Italy, [4]School of Physics, Institute of Fusion Theory and Simulation, Zhejiang University, Hangzhou, China, [5]Department of Physics and Astronomy, University of California, Irvine, CA, USA

Key Points:

- We propose and validate a model of electromagnetic ion cyclotron (EMIC) wave frequency chirping based on the Trap-Release-Amplify model of chorus waves
- The model relates EMIC wave frequency chirping to both wave intensity and background magnetic field inhomogeneity for the first time
- Observations demonstrate a clear decrease in EMIC wave chirping rate with increasing *L*-shell, consistent with the model prediction

Correspondence to:
X. Tao,
xtao@ustc.edu.cn

Citation:
An, Z., Tao, X., Zonca, F., & Chen, L. (2024). Frequency chirping of electromagnetic ion cyclotron waves in Earth's magnetosphere. *Geophysical Research Letters*, *51*, e2023GL106456. https://doi.org/10.1029/2023GL106456

Received 20 SEP 2023
Accepted 7 JAN 2024

Abstract Electromagnetic ion cyclotron (EMIC) waves are known to exhibit frequency chirping occasionally, contributing to the rapid acceleration and precipitation of energetic particles in the magnetosphere. However, the chirping mechanism of EMIC waves remains elusive. In this work, a phenomenological model of whistler mode chorus waves named the Trap-Release-Amplify (TaRA) model is applied to EMIC waves. Based on the proposed model, we explain how the chirping of EMIC waves occurs, and give predictions on their frequency chirping rates. For the first time, we relate the frequency chirping rate of EMIC waves to both the wave amplitude and the background magnetic field inhomogeneity. Direct observational evidence is provided to validate the model using previously published events of chirping EMIC waves. Our results not only provide a new model for EMIC wave frequency chirping, but more importantly, they indicate the potential wide applicability of the underlying principles of TaRA model.

Plain Language Summary Rapid change of wave frequency, or frequency chirping, can frequently be observed in space and laboratory plasmas. Chirping waves generally appear as discrete and narrowband elements and can cause rapid acceleration or scattering of energetic particles through nonlinear interactions. Correspondingly, the physical mechanism of frequency chirping has attracted considerable research interest. This work aims to explain how electromagnetic ion cyclotron (EMIC) wave frequency chirping arises, which remains an open question. We apply a previously developed model of whistler mode chorus waves named the Trap-Release-Amplify (TaRA) model to chirping EMIC waves, and make a series of chirping rate predictions. In particular, we find that after taking into account all the different stages of wave excitation, chirping rate of EMIC waves should be related to both wave amplitude and background magnetic field inhomogeneity. A comparison between the theoretical chirping rates and observations using previously published EMIC wave chirping events shows good consistency. The results provide both a new explanation for EMIC wave frequency chirping and an indirect test of the underlying principles of the TaRA model.

1. Introduction

Electromagnetic ion cyclotron (EMIC) waves have been demonstrated to play important roles in dynamics of radiation belt electrons and ring current protons. For example, scattering induced by EMIC waves is considered as one of the most important drivers of relativistic electron precipitation into the atmosphere (Blum et al., 2015; Denton et al., 2019; Drozdov et al., 2022; Hendry et al., 2017; Kersten et al., 2014; Usanova et al., 2014), via resonant (Bingley et al., 2019; Meredith et al., 2003; Ni et al., 2015; B. Wang et al., 2016), and nonresonant (X. An et al., 2022; Chen et al., 2016) wave-particle interactions. EMIC waves are also responsible for rapid decay of ring current protons during geomagnetic storms (Jordanova et al., 2001, 2007; Sakaguchi et al., 2008). Moreover, EMIC waves can transfer energy effectively between different particle populations through heating cold electrons and ions (Kitamura et al., 2018; Ma et al., 2019; Zhou et al., 2013). Correspondingly, understanding EMIC wave generation and the relevant wave-particle interaction processes could be helpful to studies about a wide range of magnetospheric phenomena.

Although the linear instability of EMIC waves is well understood and typically related to temperature anisotropy in the inner magnetosphere (Gary et al., 1996; Gendrin et al., 1984), some EMIC waves exhibit nonlinear frequency chirping, in the form of spontaneous rising-tone emissions (Mursula et al., 1994; Pickett et al., 2010).

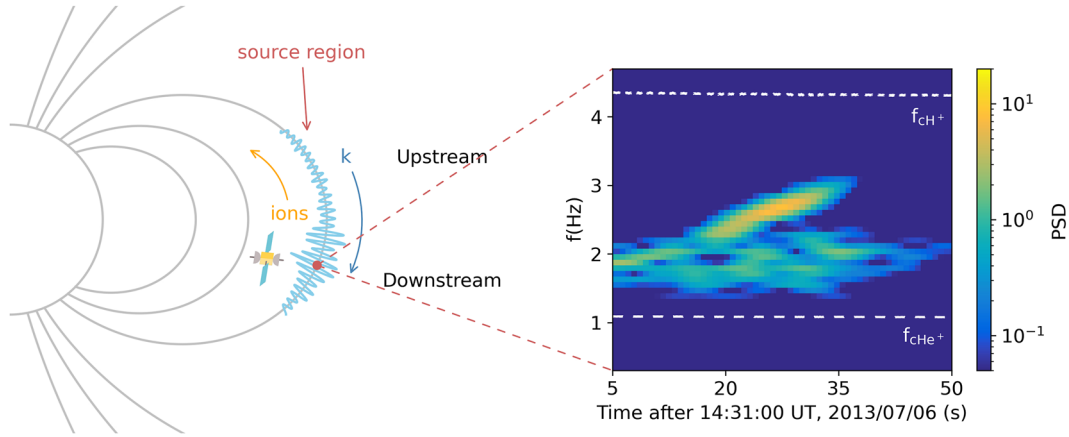

Figure 1. An illustration of our electromagnetic ion cyclotron wave frequency chirping model. As indicated by the satellite icon, chirping elements are usually observed downstream of the equator, where they have been fully amplified through nonlinear wave-particle interactions. The rising-tone element shown in the right panel was observed by RBSP-A satellite at 14:31 UT, 06 July 2013.

Such frequency chirping has also been observed in several other wave modes, including whistler mode chorus waves (Tsurutani & Smith, 1974), magnetosonic waves (Boardsen et al., 2014; Fu et al., 2014), electron cyclotron harmonic waves (S. Liu et al., 2023; Shen et al., 2021; Teng et al., 2021) in the magnetosphere and Alfvén waves (Heidbrink, 2008; Heidbrink & Sadler, 1994; McGuire et al., 1983) in fusion plasmas. These chirping waves generally consist of discrete packets that are narrowband and quasi-coherent (Tsurutani et al., 2009). Interaction with these chirping modes often results in rapid transport of energetic particles in phase space (Albert & Bortnik, 2009; Artemyev et al., 2016; Chen & Zonca, 2007; Grach & Demekhov, 2020; Grach et al., 2022; McGuire et al., 1983; Tao, Bortnik, et al., 2012; White et al., 1983; Zhang et al., 2018; Zonca et al., 2005), affecting space weather or deteriorating particle confinement in fusion devices. Therefore, there is significant research interest in understanding the physical mechanism of frequency chirping in both communities of space and laboratory plasmas.

While there are several observational studies about EMIC wave chirping (Grison et al., 2013; Mursula, 2007; Mursula et al., 1994; Nakamura et al., 2016; Pickett et al., 2010; Y. Wang et al., 2023), theoretical studies are quite limited. Hybrid simulations have clearly demonstrated that EMIC wave frequency chirping is caused by nonlinear processes (Shoji & Omura, 2013). The sequential triggering model by Omura and Nunn (2011) and Shoji et al. (2017), originally developed for chorus waves, has been applied to explain EMIC wave frequency chirping in simulations and observations (Omura et al., 2010). These studies confirmed that the frequency chirping rate is proportional to wave amplitude, a feature from the nonlinear generation process.

In this work, we propose a new model of EMIC wave frequency chirping based on the recently proposed "Trap-Release-Amplify" (TaRA) model of whistler mode chorus waves (Tao et al., 2021), considering similar nonlinear wave-particle interaction processes in the chirping of chorus and EMIC waves (Section 2). Different from previous models (Omura et al., 2010; Trakhtengerts & Demekhov, 2007), our model relates the chirping rate of EMIC waves not only to the wave amplitude but also to the background magnetic field inhomogeneity. Two chirping rate predictions are given in Section 2 and compared with observations in Section 3. The comparison shows good agreement, suggesting the validity of our model and that the same underlying principle exists between chorus wave and EMIC wave frequency chirping. Our results, therefore, not only provide a different way of understanding EMIC wave frequency chirping but also give new insights into the chirping mechanisms of other wave modes in both space and laboratory plasmas.

2. A Model of EMIC Wave Frequency Chirping

We illustrate our chirping model of EMIC waves in Figure 1. Each element of the chirping EMIC wave is represented by a narrowband quasi-coherent wave packet, with a frequency that increases nearly continuously from ω_{min} to ω_{max}. We further adopt the basic principle of the TaRA model of chorus and divide the generation region of

EMIC waves into upstream and downstream regions separated by the equator. As the generated part of the EMIC wave packet propagates downstream of the equator, it constantly encounters fresh resonant ions moving in the opposite direction. If the wave is quasi-coherent and intense enough, some of the ions will get phase-trapped by the wave packet. Because of Liouville's theorem, the phase space density along a particle's trajectory is conserved. The resonant interaction between ions and EMIC waves results in phase-trapped ions moving from low phase space density region to high phase space density region, forming a localized phase space hole (Nunn, 1974; Tao et al., 2020), which has been demonstrated by computer simulations in Shoji and Omura (2011) and Shoji and Omura (2013). As the ions travel across the wave packet, they will eventually get released in the upstream region where the wave amplitude is small. However, these released ions still retain certain phase correlation, resulting in a current and selective amplification of new emissions from the nearly continuous spectrum of background EMIC waves. The condition for the selective amplification is mathematically expressed using the phase-locking condition $\mathrm{d}^2\zeta/\mathrm{d}t^2 = 0$. Here, ζ is the wave-particle interaction phase angle between the wave magnetic field $\delta\mathbf{B}$ and the ion perpendicular velocity $\mathbf{v}_\perp$ with respect to the background magnetic field. Such a selection rule guarantees maximum power transfer from ions to waves by holding the resonance condition $\mathrm{d}\zeta/\mathrm{d}t = 0$ for the longest time possible. Note that fresh ions are continuously entrapped in the downstream and detrapped in the upstream, allowing frequency chirping from $\omega_{\min}$ to $\omega_{\max}$.

Based on the above chirping model, two different chirping rates can then be derived. From the nonlinear wave-particle interaction theories of parallel propagating EMIC waves, the second-order time derivative of the wave-particle interaction phase angle ζ could be written as (Omura et al., 2010)

$$\frac{\mathrm{d}^2\zeta}{\mathrm{d}t^2} = \omega_{tr}^2 \sin\zeta + (R_1 + R_2), \tag{1}$$

where

$$R_1 = \left(1 - \frac{v_r}{v_g}\right)^2 \frac{\partial\omega}{\partial t}, \tag{2}$$

$$R_2 = \left[\left(\frac{v_\perp^2}{2v_p} + \frac{v_r^2}{v_g}\right)\frac{\omega}{\Omega_i} - v_r\right]\frac{\partial\Omega_i}{\partial s}, \tag{3}$$

assuming constant cold plasma density along the field line. Here R_1 and R_2 represent the effects of frequency chirping and background magnetic field nonuniformity, respectively, and s is the distance along a field line from the equator. The parameter R, widely used by other studies (Nunn, 1974; Vomvoridis & Denavit, 1979), equals $(R_1 + R_2)/\omega_{tr}^2$. In Equation 1 above, $\omega_{tr} = \sqrt{kv_\perp\Omega_w}$ is the phase-trapping frequency, with k the wavenumber and $\Omega_w \equiv q_i\delta B/m_i c$. Here q_i is the ion charge, m_i is the ion mass and c is the speed of light in vacuum. In Equations 2 and 3, $v_r = (\omega - \Omega_i)/k$ is the cyclotron resonance velocity, $v_g = \partial\omega/\partial k$ is the wave group velocity, $v_p = \omega/k$ is wave phase velocity, and $\Omega_i \equiv q_i B/m_i c$ is the non-relativistic ion cyclotron frequency.

The first chirping rate is deducted from nonlinear wave-particle interaction theories and is same as the one obtained by the previous model of EMIC wave chirping. At the equator, $R_2 \propto \partial\Omega_i/\partial s \sim 0$. We then arrive at the relation between chirping rates and wave amplitudes as in earlier studies (Omura et al., 2008, 2010; Vomvoridis et al., 1982; Zonca et al., 2022):

$$\frac{\partial\omega}{\partial t} = R\left(1 - \frac{v_r}{v_g}\right)^{-2}\omega_{tr}^2\Big|_{s=0} \propto \delta B. \tag{4}$$

Effective power transfer is found to occur for R to be about 0.5 (Omura et al., 2008; Vomvoridis et al., 1982; Zonca et al., 2021). This chirping rate has been obtained before, and for convenience, it will be called the nonlinear chirping rate.

Applying the principle of the TaRA model of chorus to EMIC waves allows us to obtain a new expression of the chirping rate. At the upstream source location s_0, phase-trapped ions are released to amplify new waves from the pre-existing thermal noise spectrum, which means that δB is small or ω_{tr}^2 is negligible compared with R_2 in Equation 1. The phase-locking condition is then reduced to

$$\frac{d^2\zeta}{dt^2} \approx R_1 + R_2 = 0, \tag{5}$$

leading to

$$\frac{\partial\omega}{\partial t} = -\left(1 - \frac{v_r}{v_g}\right)^{-2}\left[\left(\frac{v_\perp^2}{2v_p} + \frac{v_r^2}{v_g}\right)\frac{\omega}{\Omega_i} - v_r\right]\frac{\partial\Omega_i}{\partial s}\bigg|_{s=s_0}. \tag{6}$$

This equation demonstrates the dependence of chirping rate on background magnetic field inhomogeneity and is expected to be evaluated at the wave source location upstream of the equator. An order-of-magnitude estimate of the source location s_0 is that $s_0 = (2\pi|v_r|/\xi\Omega_{i0})^{1/3}$ (Helliwell, 1967), corresponding to a shift of π radian of the wave particle interaction phase angle ζ from the equator assuming linear motion of ions. Here we approximate the background magnetic field B near the equator as $B = B_0(1 + \xi s^2)$, and ξ is a measure of the magnetic field inhomogeneity.

So far, two chirping rate expressions have been derived: Equation 4 at the equator and Equation 6 in the source location s_0. The new model of EMIC wave chirping, therefore, predicts that the chirping rate of EMIC waves is not only related to wave amplitude at the equator, but also to the background magnetic inhomogeneity. We must emphasize that, although the two equations look different and have different origins of physical mechanisms, they are consistent and both are correct at different stages of wave excitation.

3. Comparing the Model to Observations

We now provide a direct comparison with observations to test the above two EMIC wave chirping rate predictions using all the previously published events we are aware of. Different from whistler mode chorus waves, there are not many observed events of chirping EMIC waves. The only selection rule we apply is that the magnetic latitude of the event should be less than 5° for Equation 4 and less than 10° for Equation 6 to avoid being too far away from the equator. We select events closer to the equator for Equation 4 because wave amplitude could vary significantly as wave propagates from the equator to high latitudes. In total, we have 15 EMIC wave rising-tones for Equation 6 and 11 for Equation 4, all of which are in-situ observations of spontaneously excited EMIC waves with clear frequency chirping elements. These observations were made by different spacecraft including Cluster (Escoubet et al., 1997), Van Allen Probes (Mauk et al., 2013), and Time History of Events and Macroscale Interactions during Substorms (THEMIS, Angelopoulos (2008)), during different time periods and at a wide range of radial distances. Therefore, these selected events should be a good representation of EMIC wave chirping elements in the magnetosphere. Their brief information is summarized in Table 1.

Before calculating the theoretical chirping rates, we describe the method we use to estimate wavenumber k. Although it is typical to obtain k from the cold plasma dispersion relation, this approach could become very inaccurate at frequencies near ion gyrofrequencies. Furthermore, the heavy ion (He^+ and O^+) densities are sometimes difficult to determine or even missing in satellite data. Using empirical heavy ion compositions is inappropriate here, as different events might correspond to very different cold plasma parameters. To avoid this problem, we adopt the wavenumber analysis method proposed by Chen et al. (2019), which allows us to extract $k(\omega)$ directly from the observed waveforms. The method involves three steps for a chirping element like the one shown in Figure 2a. First, we determine the evolution of wave frequency with time from the wave spectrogram. In this step, we only select points with large enough power spectral densities and small enough wave normal angles. Specifically, we require that magnetic power spectral density $PSD > 0.01PSD_{max}$, in which PSD_{max} is the maximum PSD in the chirping element, and wave normal angle $\Psi < 45°$. The selected points are shown in Figure 2b. Second, we use the singular value decomposition method (Santolík et al., 2003) to solve for k at the selected points, using five components of the electromagnetic fields (B_x, B_y, B_z, E_y, and E_z, in the GSE coordinate system). The results are plotted against ω in Figure 2c. Finally, we fit all the points with a quadratic function: $k = a\omega^2 + b\omega + c$ to obtain a single wavenumber at a certain frequency. For a particular element, we use $\omega_{mid} = (\omega_{min} + \omega_{max})/2$ and the corresponding $k(\omega_{mid})$ to estimate its theoretical chirping rate. This method of estimating $\boldsymbol{k}$ does not rely on the information of plasma components; however, one potential concern is that antennas onboard spacecraft actually measure $\boldsymbol{E}/Z$, where Z is the complex transfer function of the interface between the electric antennas and the plasma. Santolík and Parrot (2000) and Parrot et al. (2001) demonstrated that Z is highly variable and

Table 1
Brief Information of the 15 Observational Events, Arranged in the Order of Time of Occurrence, Which Is a 10-Minute-Long Vicinity of the Interested Cirping Element

	Time of occurrence (UT)	*L*-shell	MLT (hr)	MLAT (deg)	Frequency range (Hz)	Observed by	First reported by
1	07:55–08:05, 2002/03/30	4.45	22.3	−3.4	1.56–2.87	Cluster 4	Pickett et al. (2010)
2	00:10–00:20, 2003/03/27	4.17	22.6	−1.78	1.6–3.46	Cluster 4	Grison et al. (2013)
3	09:05–09:15, 2008/04/16	7.2	17.8	−8.82	0.31–0.59	THEMIS A	Nakamura et al. (2015)
4	17:40–17:50, 2008/10/11	6.98	12	0.2	0.5–0.97	THEMIS A	Nakamura et al. (2015)
5	18:30–18:40, 2010/06/25	8.03	17.6	0.08	0.28–0.5	THEMIS A	Nakamura et al. (2015)
6	17:35–17:45, 2010/07/11	7.83	16.5	3.7	0.38–0.63	THEMIS E	Nakamura et al. (2014)
7	14:20–14:30, 2010/09/09	8.33	13.2	4.83	0.5–0.97	THEMIS D	Nakamura et al. (2014)
8	13:20–13:30, 2010/09/24	8.27	12.4	4.8	0.47–0.84	THEMIS D	Nakamura et al. (2015)
9	08:35–08:45, 2011/09/25	8.87	17.9	−2.9	0.25–0.41	THEMIS A	Nakamura et al. (2015)
10	14:25–14:35, 2013/07/06	4.05	18.1	2.45	2.25–3.13	RBSP-A	Chen et al. (2019)
11	19:50–20:00, 2013/11/29	5.78	15	2.82	0.31–0.45	RBSP-B	Y. Wang et al. (2023)
12	11:30–11:40, 2014/02/23	6.68	14.9	−1.54	0.75–1.19	THEMIS D	N. Liu et al. (2020)
13	23:35–23:45, 2014/05/04	5.83	9.99	−5.03	0.94–1.5	RBSP-A	Y. Wang et al. (2023)
14	10:15–10:25, 2015/12/22	5.4	13.3	−8.02	1.06–1.94	RBSP-A	Sigsbee et al. (2020)
15	12:15–12:25, 2017/09/07	5.68	13.7	5.63	0.88–1.75	RBSP-A	Zhu et al. (2020)

Note. Event 11 is a helium-band wave, while the others are hydrogen-band waves.

event-dependent for waves above 1 kHz. On the other hand, for EMIC waves with frequencies around 1 Hz, Grison et al. (2014) concluded that $Z \approx 1$ is appropriate for Cluster data. As this $Z \approx 1$ value is also consistent with the Van Allen Probes results of Chen et al. (2019), it is also the assumption adopted by our study.

Figure 3 shows comparisons between observational (Γ_{ob}) and theoretical chirping rates. Figure 3a shows the comparison for $\Gamma(\delta B)$, Equation 4, and Figure 3b for $\Gamma(\partial B/\partial s)$, Equation 6. When estimating the theoretical chirping rates, we calculate δB by integrating over the wave power spectral density. Both the equatorial value B_0 and the inhomogeneity factor ξ of the background magnetic field are derived by fitting data given by the T89 magnetic field model (Tsyganenko, 1989) with a parabolic function $B = B_0(1 + \xi s^2)$. The perpendicular velocity $v_\perp$ is estimated from the resonant velocity v_r and a pitch angle $\alpha = 70°$, following that nonlinear phase-trapping occurs most easily for pitch angles between 65° and 75° (Inan et al., 1978). For observational chirping rates, we simply use $\Gamma_{ob} = (\omega_{max} - \omega_{min})/\Delta t$ with Δt the duration of element. Each point represents an event in Table 1, with the corresponding satellite missions and *L*-shell values categorized by different markers and colors, respectively. The shaded region represents a maximum difference of a factor of two. Figure 3 shows that, for most events (8 out of 11 for Figure 3a and 13 out of 15 for Figure 3b), the differences between observation and both theoretical

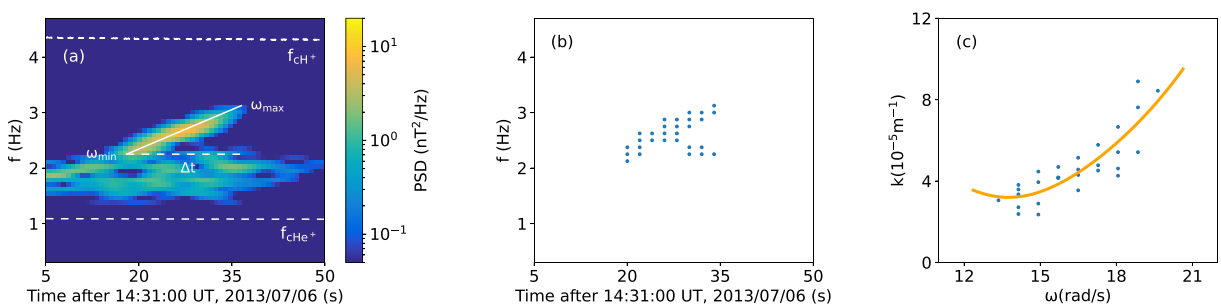

Figure 2. A demonstration of the wavenumber estimation method. (a) The spectrogram of the chirping element, Event 10 of Table 1. (b) Points in the spectrogram which satisfy all selection rules described in the text. (c) Wavenumber k solved with the singular value decomposition method (the blue dots) and a quadratic fit (the orange curve) of them as a function of frequency ω. The minimum and maximum frequency of the element are denoted by ω_{min} and ω_{max}, respectively, and the duration of the element is denoted by Δt in panel (a).

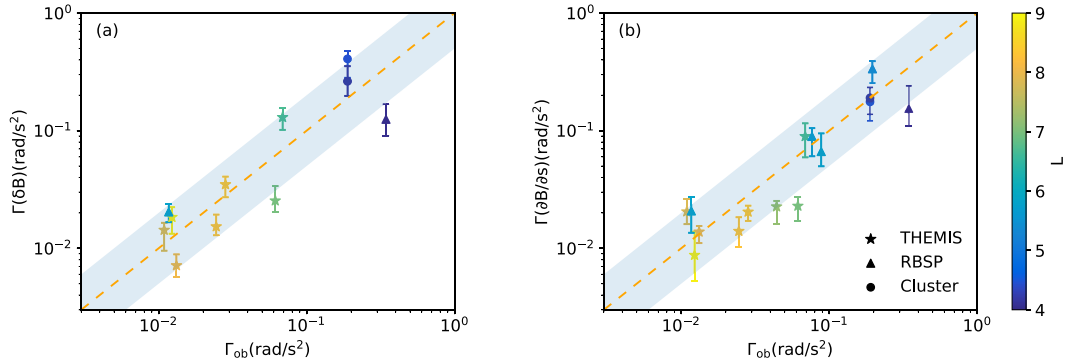

Figure 3. Comparisons between observational (Γ_{ob}) and theoretical chirping rates calculated with (a) Equation 4 $\Gamma(\delta B)$ and (b) Equation 6, $\Gamma(\partial B/\partial s)$. Different colors and markers categorize the L-shell value and data source of each case, respectively. The shadowed region is confined by lines $\Gamma = \Gamma_{ob}/2$ and $2\Gamma_{ob}$, while the orange dashed line denotes $\Gamma = \Gamma_{ob}$. Error bars indicate the range of Γ as pitch angle α varies from 65° to 75°; the markers are calculated at exactly $\alpha = 70°$.

chirping rates are less than a factor of two. The maximum difference for all events is less than a factor of three (not shown). Correspondingly, the direct comparison presented in Figure 3 demonstrates very good agreement between the new model and previously published observations. Furthermore, similar to chorus waves (Tao, Li, et al., 2012; Tao et al., 2014; Xie et al., 2021), we can see a decrease of chirping rate as L increases because of smaller magnetic field inhomogeneity at larger L-shells.

The discrepancies between observations and theoretical predictions come mainly from uncertainties in some parameters, such as wave amplitude (δB), the nonlinear parameter R, the pitch angle α, and source location (s_0). Although we select events with $|\mathrm{MLAT}| < 5°$ when calculating δB, the wave amplitude might still be different from its equatorial value, and the parameter R might take a value different from 0.5 (Tao et al., 2017; Teng et al., 2023). As an example, we show the uncertainty of theoretical chirping rates caused by varying the pitch angle α from 65° to 75° in Figure 3. Furthermore, the equation $s_0 = (2\pi|v_r|/\xi\Omega_{i0})^{1/3}$ we use to estimate the source location is only an estimation to the lowest order by assuming adiabatic motions of ions. To be exact, the release location needs to be calculated by taking full nonlinear wave particle interactions into consideration (Tao et al., 2021; Y. Wu et al., 2022). Other potential causes of estimation errors include the assumption of constant cold plasma density along the field line, and the fitting of $k(\omega)$. In general, taking these possible sources of uncertainties into consideration, we conclude that good agreement between observations and two different yet consistent theoretical chirping rate estimates has been reached. Therefore, the model proposed in Section 2 could well explain the chirping of EMIC waves in a different way from previous ones (Omura et al., 2010; Trakhtengerts & Demekhov, 2007).

4. Summary

In this work, we presented a new model of EMIC wave chirping and directly compared it with in situ satellite observations. The two theoretical predictions of chirping rates exhibit good agreement with observations, indicating that both rates are manifestations of the same underlying process at different stages of wave packet propagation. The new model not only relates EMIC wave chirping to wave amplitude at the equator but also to background magnetic field inhomogeneity, which is a novel contribution. The new chirping rate allows an easy explanation of the dependence of EMIC wave chirping rate on L-shell in the magnetosphere. Combining both predictions also opens up new possibilities. For example, we may estimate wave amplitude of rising-tone EMIC waves directly from the background magnetic field inhomogeneity (Z. Wu et al., 2023).

Furthermore, our comparison confirms that the principle of the TaRA model, initially developed for whistler mode chorus, is equally applicable to EMIC wave chirping. We note that some components of the TaRA model, such as phase-locking and detrapping, are also shared by Alfvén wave chirping in fusion plasmas from a recent study (X. Wang et al., 2022). Combining these findings suggests the possibility of a unified theoretical framework to explain the nonlinear chirping of different waves in various plasma environments (Chen & Zonca, 2016; Zonca et al., 2022).

Data Availability Statement

The electromagnetic field data used in this work are provided by Cluster, THEMIS, and Van Allen Probes satellites, and can be found at Z. An (2023).

Acknowledgments
This work was supported by the B-type Strategic Priority Program of the Chinese Academy of Sciences, Grant XDB41000000, NSFC Grants (42174182 and 11235009), National Key R&D Program of China (2022YFF0503702), and Euratom Research and Training Programme (Grant 101052200—EUROfusion). Views and opinions expressed are however those of the author(s) only and do not necessarily reflect those of the European Union or the European Commission.

References

Albert, J. M., & Bortnik, J. (2009). Nonlinear interaction of radiation belt electrons with electromagnetic ion cyclotron waves. *Geophysical Research Letters*, *36*(12), L12110. https://doi.org/10.1029/2009GL038904

An, X., Artemyev, A., Angelopoulos, V., Zhang, X., Mourenas, D., & Bortnik, J. (2022). Nonresonant scattering of relativistic electrons by electromagnetic ion cyclotron waves in Earth's radiation belts. *Physical Review Letters*, *129*(13), 135101. https://doi.org/10.1103/PhysRevLett.129.135101

An, Z. (2023). Dataset of "Frequency chirping of electromagnetic ion cyclotron waves in Earth's magnetosphere". https://doi.org/10.5281/zenodo.8365251

Angelopoulos, V. (2008). The THEMIS mission. *Space Science Reviews*, *141*(5), 5–34. https://doi.org/10.1007/s11214-008-9336-1

Artemyev, A. V., Neishtadt, A. I., Vasiliev, A. A., & Mourenas, D. (2016). Kinetic equation for nonlinear resonant wave-particle interaction. *Physics of Plasmas*, *23*(9), 090701. https://doi.org/10.1063/1.4962526

Bingley, L., Angelopoulos, V., Sibeck, D., Zhang, X., & Halford, A. (2019). The evolution of a pitch-angle "bite-out" scattering signature caused by EMIC wave activity: A case study. *Journal of Geophysical Research: Space Physics*, *124*(7), 5042–5055. https://doi.org/10.1029/2018JA026292

Blum, L. W., Halford, A., Millan, R., Bonnell, J. W., Goldstein, J., Usanova, M., et al. (2015). Observations of coincident EMIC wave activity and duskside energetic electron precipitation on 18-19 January 2013. *Geophysical Research Letters*, *42*(14), 5727–5735. https://doi.org/10.1002/2015GL065245

Boardsen, S. A., Hospodarsky, G. B., Kletzing, C. A., Pfaff, R. F., Kurth, W. S., Wygant, J. R., & MacDonald, E. A. (2014). Van Allen Probe observations of periodic rising frequencies of the fast magnetosonic mode. *Geophysical Research Letters*, *41*(23), 8161–8168. https://doi.org/10.1002/2014GL062020

Chen, L., Thorne, R. M., Bortnik, J., & Zhang, X.-J. (2016). Nonresonant interactions of electromagnetic ion cyclotron waves with relativistic electrons. *Journal of Geophysical Research: Space Physics*, *121*(10), 9913–9925. https://doi.org/10.1002/2016JA022813

Chen, L., Zhu, H., & Zhang, X. (2019). Wavenumber analysis of EMIC waves. *Geophysical Research Letters*, *46*(11), 5689–5697. https://doi.org/10.1029/2019GL082686

Chen, L., & Zonca, F. (2007). Theory of Alfvén waves and energetic particle physics in burning plasmas. *Nuclear Fusion*, *47*(10), S727–S734. https://doi.org/10.1088/0029-5515/47/10/S20

Chen, L., & Zonca, F. (2016). Physics of Alfvén waves and energetic particles in burning plasmas. *Reviews of Modern Physics*, *88*(1), 015008. https://doi.org/10.1103/RevModPhys.88.015008

Denton, R. E., Ofman, L., Shprits, Y. Y., Bortnik, J., Millan, R. M., Rodger, C. J., et al. (2019). Pitch angle scattering of sub-MeV relativistic electrons by electromagnetic ion cyclotron waves. *Journal of Geophysical Research: Space Physics*, *124*(7), 5610–5626. https://doi.org/10.1029/2018JA026384

Drozdov, A. Y., Allison, H. J., Shprits, Y. Y., Usanova, M. E., Saikin, A., & Wang, D. (2022). Depletions of multi-MeV electrons and their association to minima in phase space density. *Geophysical Research Letters*, *49*(8), e2021GL097620. https://doi.org/10.1029/2021GL097620

Escoubet, C. P., Schmidt, R., & Goldstein, M. L. (1997). Cluster—Science and mission overview. *Space Science Reviews*, *79*(1/2), 11–32. https://doi.org/10.1023/A:1004923124586

Fu, H. S., Cao, J. B., Zhima, Z., Khotyaintsev, Y. V., Angelopoulos, V., Santolík, O., et al. (2014). First observation of rising-tone magnetosonic waves. *Geophysical Research Letters*, *41*(21), 7419–7426. https://doi.org/10.1002/2014GL061867

Gary, S. P., Vazquez, V. M., & Winske, D. (1996). Electromagnetic proton cyclotron instability: Proton velocity distributions. *Journal of Geophysical Research*, *101*(A6), 13327–13334. https://doi.org/10.1029/96JA00295

Gendrin, R., Ashour-Abdalla, M., Omura, Y., & Quest, K. (1984). Linear analysis of ion cyclotron interaction in a multicomponent plasma. *Journal of Geophysical Research*, *89*(A10), 9119–9124. https://doi.org/10.1029/JA089iA10p09119

Grach, V. S., Artemyev, A. V., Demekhov, A. G., Zhang, X.-J., Bortnik, J., Angelopoulos, V., et al. (2022). Relativistic electron precipitation by EMIC waves: Importance of nonlinear resonant effects. *Geophysical Research Letters*, *49*(17), e2022GL099994. https://doi.org/10.1029/2022GL099994

Grach, V. S., & Demekhov, A. G. (2020). Precipitation of relativistic electrons under resonant interaction with electromagnetic ion cyclotron wave packets. *Journal of Geophysical Research: Space Physics*, *125*(2), e2019JA027358. https://doi.org/10.1029/2019JA027358

Grison, B., Escoubet, C. P., Santolík, O., Cornilleau-Wehrlin, N., & Khotyaintsev, Y. (2014). Wave number determination of Pc 1-2 mantle waves considering He++ ions: A cluster study. *Journal of Geophysical Research: Space Physics*, *119*(9), 7601–7614. https://doi.org/10.1002/2013JA019719

Grison, B., Santolík, O., Cornilleau-Wehrlin, N., Masson, A., Engebretson, M. J., Pickett, J. S., et al. (2013). Emic triggered chorus emissions in cluster data. *Journal of Geophysical Research: Space Physics*, *118*(3), 1159–1169. https://doi.org/10.1002/jgra.50178

Heidbrink, W. W. (2008). Basic physics of Alfvén instabilities driven by energetic particles in toroidally confined plasmas. *Physics of Plasmas*, *15*(5), 055501. https://doi.org/10.1063/1.2838239

Heidbrink, W. W., & Sadler, G. J. (1994). The behaviour of fast ions in tokamak experiments. *Nuclear Fusion*, *34*(4), 535–615. https://doi.org/10.1088/0029-5515/34/4/I07

Helliwell, R. A. (1967). A theory of discrete VLF emissions from the magnetosphere. *Journal of Geophysical Research*, *72*(19), 4773–4790. https://doi.org/10.1029/JZ072i019p04773

Hendry, A. T., Rodger, C. J., & Clilverd, M. A. (2017). Evidence of sub-MeV EMIC-driven electron precipitation. *Geophysical Research Letters*, *44*(3), 1210–1218. https://doi.org/10.1002/2016GL071807

Inan, U. S., Bell, T. F., & Helliwell, R. A. (1978). Nonlinear pitch angle scattering of energetic electrons by coherent VLF waves in the magnetosphere. *Journal of Geophysical Research*, *83*(A7), 3235–3253. https://doi.org/10.1029/JA083iA07p03235

Jordanova, V. K., Farrugia, C. J., Thorne, R. M., Khazanov, G. V., Reeves, G. D., & Thomsen, M. F. (2001). Modeling ring current proton precipitation by electromagnetic ion cyclotron waves during the May 14–16, 1997, storm. *Journal of Geophysical Research*, *106*(A1), 7–22. https://doi.org/10.1029/2000JA002008

Jordanova, V. K., Spasojevic, M., & Thomsen, M. F. (2007). Modeling the electromagnetic ion cyclotron wave-induced formation of detached subauroral proton arcs. *Journal of Geophysical Research*, *112*(A8), A08209. https://doi.org/10.1029/2006JA012215

Kersten, T., Horne, R. B., Glauert, S. A., Meredith, N. P., Fraser, B. J., & Grew, R. S. (2014). Electron losses from the radiation belts caused by EMIC waves. *Journal of Geophysical Research: Space Physics*, *119*(11), 8820–8837. https://doi.org/10.1002/2014JA020366

Kitamura, N., Kitahara, M., Shoji, M., Miyoshi, Y., Hasegawa, H., Nakamura, S., et al. (2018). Direct measurements of two-way wave-particle energy transfer in a collisionless space plasma. *Science*, *361*(6406), 1000–1003. https://doi.org/10.1126/science.aap8730

Liu, N., Su, Z., Gao, Z., Zheng, H., Wang, Y., & Wang, S. (2020). Can solar wind decompressive discontinuities suppress magnetospheric electromagnetic ion cyclotron waves associated with fresh proton injections? *Geophysical Research Letters*, *47*(17), e2020GL090296. https://doi.org/10.1029/2020GL090296

Liu, S., Chen, Y., Yang, Q., Yang, H., Xiao, F., Wang, B., & Gao, Z. (2023). Statistical study on spatial distribution of frequency-chirping ECH elements by Van Allen Probes. *Geophysical Research Letters*, *50*(22), e2023GL106371. https://doi.org/10.1029/2023GL106371

Ma, Q., Li, W., Yue, C., Thorne, R. M., Bortnik, J., Kletzing, C. A., et al. (2019). Ion heating by electromagnetic ion cyclotron waves and magnetosonic waves in the Earth's inner magnetosphere. *Geophysical Research Letters*, *46*(12), 6258–6267. https://doi.org/10.1029/2019GL083513

Mauk, B. H., Fox, N. J., Kanekal, S. G., Kessel, R. L., Sibeck, D. G., & Ukhorskiy, A. (2013). Science objectives and rationale for the radiation belt storm probes mission. *Space Science Reviews*, *179*(1–4), 3–27. https://doi.org/10.1007/s11214-012-9908-y

McGuire, K., Goldston, R., Bell, M., Bitter, M., Bol, K., Brau, K., et al. (1983). Study of high-beta magnetohydrodynamic modes and fast-ion losses in PDX. *Physical Review Letters*, *50*(12), 891–895. https://doi.org/10.1103/PhysRevLett.50.891

Meredith, N. P., Thorne, R. M., Horne, R. B., Summers, D., Fraser, B. J., & Anderson, R. R. (2003). Statistical analysis of relativistic electron energies for cyclotron resonance with EMIC waves observed on CRRES. *Journal of Geophysical Research*, *108*(A6), 1250. https://doi.org/10.1029/2002JA009700

Mursula, K. (2007). Satellite observations of Pc 1 pearl waves: The changing paradigm. *Journal of Atmospheric and Solar-Terrestrial Physics*, *69*(14), 1623–1634. https://doi.org/10.1016/j.jastp.2007.02.013

Mursula, K., Blomberg, L. G., Lindqvist, P. A., Marklund, G. T., Bräysy, T., Rasinkangas, R., & Tanskanen, P. (1994). Dispersive Pc1 bursts observed by Freja. *Geophysical Research Letters*, *21*(17), 1851–1854. https://doi.org/10.1029/94GL01584

Nakamura, S., Omura, Y., & Angelopoulos, V. (2016). A statistical study of EMIC rising and falling tone emissions observed by THEMIS. *Journal of Geophysical Research: Space Physics*, *121*(9), 8374–8391. https://doi.org/10.1002/2016JA022353

Nakamura, S., Omura, Y., Machida, S., Shoji, M., Nosé, M., & Angelopoulos, V. (2014). Electromagnetic ion cyclotron rising tone emissions observed by THEMIS probes outside the plasmapause. *Journal of Geophysical Research: Space Physics*, *119*(3), 1874–1886. https://doi.org/10.1002/2013JA019146

Nakamura, S., Omura, Y., Shoji, M., Nosé, M., Summers, D., & Angelopoulos, V. (2015). Subpacket structures in EMIC rising tone emissions observed by the THEMIS probes. *Journal of Geophysical Research: Space Physics*, *120*(9), 7318–7330. https://doi.org/10.1002/2014JA020764

Ni, B., Cao, X., Zou, Z., Zhou, C., Gu, X., Bortnik, J., et al. (2015). Resonant scattering of outer zone relativistic electrons by multiband EMIC waves and resultant electron loss time scales. *Journal of Geophysical Research: Space Physics*, *120*(9), 7357–7373. https://doi.org/10.1002/2015JA021466

Nunn, D. (1974). A self-consistent theory of triggered VLF emissions. *Planetary and Space Science*, *22*(3), 349–378. https://doi.org/10.1016/0032-0633(74)90070-1

Omura, Y., Katoh, Y., & Summers, D. (2008). Theory and simulation of the generation of whistler-mode chorus. *Journal of Geophysical Research*, *113*(A4), A04223. https://doi.org/10.1029/2007JA012622

Omura, Y., & Nunn, D. (2011). Triggering process of whistler mode chorus emissions in the magnetosphere. *Journal of Geophysical Research*, *116*(A5), A05205. https://doi.org/10.1029/2010JA016280

Omura, Y., Pickett, J., Grison, B., Santolík, O., Dandouras, I., Engebretson, M., et al. (2010). Theory and observation of electromagnetic ion cyclotron triggered emissions in the magnetosphere. *Journal of Geophysical Research*, *115*(A7), A07234. https://doi.org/10.1029/2010JA015300

Parrot, M., Lefeuvre, F., Rauch, J. L., Santolìk, O., & Mogilevski, M. M. (2001). Propagation characteristics of auroral kilometric radiation observed by the MEMO experiment on Interball 2. *Journal of Geophysical Research*, *106*(A1), 315–325. https://doi.org/10.1029/2000JA900072

Pickett, J. S., Grison, B., Omura, Y., Engebretson, M. J., Dandouras, I., Masson, A., et al. (2010). Cluster observations of EMIC triggered emissions in association with Pc1 waves near Earth's plasmapause. *Geophysical Research Letters*, *37*(9), L09104. https://doi.org/10.1029/2010GL042648

Sakaguchi, K., Shiokawa, K., Miyoshi, Y., Otsuka, Y., Ogawa, T., Asamura, K., & Connors, M. (2008). Simultaneous appearance of isolated auroral arcs and Pc 1 geomagnetic pulsations at subauroral latitudes. *Journal of Geophysical Research*, *113*(A5), A05201. https://doi.org/10.1029/2007JA012888

Santolík, O., & Parrot, M. (2000). Application of wave distribution function methods to an ELF hiss event at high latitudes. *Journal of Geophysical Research*, *105*(A8), 18885–18894. https://doi.org/10.1029/2000JA900029

Santolík, O., Parrot, M., & Lefeuvre, F. (2003). Singular value decomposition methods for wave propagation analysis. *Radio Science*, *38*(1), 1010. https://doi.org/10.1029/2000RS002523

Shen, X.-C., Li, W., & Ma, Q. (2021). Periodic rising and falling tone ECH waves from Van Allen Probes observations. *Geophysical Research Letters*, *48*(7), e2020GL091330. https://doi.org/10.1029/2020GL091330

Shoji, M., Miyoshi, Y., Katoh, Y., Keika, K., Angelopoulos, V., Kasahara, S., et al. (2017). Ion hole formation and nonlinear generation of electromagnetic ion cyclotron waves: THEMIS observations. *Geophysical Research Letters*, *44*(17), 8730–8738. https://doi.org/10.1002/2017GL074254

Shoji, M., & Omura, Y. (2011). Simulation of electromagnetic ion cyclotron triggered emissions in the Earth's inner magnetosphere. *Journal of Geophysical Research*, *116*(A5), A05212. https://doi.org/10.1029/2010JA016351

Shoji, M., & Omura, Y. (2013). Triggering process of electromagnetic ion cyclotron rising tone emissions in the inner magnetosphere. *Journal of Geophysical Research: Space Physics*, *118*(9), 5553–5561. https://doi.org/10.1002/jgra.50523

Sigsbee, K., Kletzing, C. A., Faden, J. B., Jaynes, A. N., Reeves, G. D., & Jahn, J. (2020). Simultaneous observations of electromagnetic ion cyclotron (EMIC) waves and pitch angle scattering during a Van Allen Probes conjunction. *Journal of Geophysical Research: Space Physics*, *125*(4), e2019JA027424. https://doi.org/10.1029/2019JA027424

Tao, X., Bortnik, J., Thorne, R. M., Albert, J., & Li, W. (2012). Effects of amplitude modulation on nonlinear interactions between electrons and chorus waves. *Geophysical Research Letters*, *39*(6), L06102. https://doi.org/10.1029/2012GL051202

Tao, X., Li, W., Bortnik, J., Thorne, R. M., & Angelopoulos, V. (2012). Comparison between theory and observation of the frequency sweep rates of equatorial rising tone chorus. *Geophysical Research Letters*, *39*(8), L08106. https://doi.org/10.1029/2012GL051413

Tao, X., Lu, Q., Wang, S., & Dai, L. (2014). Effects of magnetic field configuration on the day-night asymmetry of chorus occurrence rate: A numerical study. *Geophysical Research Letters*, *41*(19), 6577–6582. https://doi.org/10.1002/2014GL061493

Tao, X., Zonca, F., & Chen, L. (2017). Investigations of the electron phase space dynamics in triggered whistler wave emissions using low noise δf method. *Plasma Physics and Controlled Fusion*, *59*(9), 094001. https://doi.org/10.1088/1361-6587/aa759a

Tao, X., Zonca, F., & Chen, L. (2021). A "Trap-Release-Amplify" model of chorus waves. *Journal of Geophysical Research: Space Physics*, *126*(9), e2021JA029585. https://doi.org/10.1029/2021JA029585

Tao, X., Zonca, F., Chen, L., & Wu, Y. (2020). Theoretical and numerical studies of chorus waves: A review. *Science China Earth Sciences*, *63*(1), 78–92. https://doi.org/10.1007/s11430-019-9384-6

Teng, S., Wu, Y., Guo, R., Yao, Z., & Tao, X. (2021). Observation of periodic rising and falling tone ECH waves at Saturn. *Geophysical Research Letters*, *48*(15), e2021GL094559. https://doi.org/10.1029/2021GL094559

Teng, S., Wu, Y., Harada, Y., Bortnik, J., Zonca, F., Chen, L., & Tao, X. (2023). Whistler-mode chorus waves at Mars. *Nature Communications*, *14*(1), 3142. https://doi.org/10.1038/s41467-023-38776-z

Trakhtengerts, V. Y., & Demekhov, A. G. (2007). Generation of Pc 1 pulsations in the regime of backward wave oscillator. *Journal of Atmospheric and Solar-Terrestrial Physics*, *69*(14), 1651–1656. https://doi.org/10.1016/j.jastp.2007.02.009

Tsurutani, B. T., & Smith, E. J. (1974). Postmidnight chorus: A substorm phenomenon. *Journal of Geophysical Research*, *79*(1), 118–127. https://doi.org/10.1029/JA079i001p00118

Tsurutani, B. T., Verkhoglyadova, O. P., Lakhina, G. S., & Yagitani, S. (2009). Properties of dayside outer zone chorus during HILDCAA events: Loss of energetic electrons. *Journal of Geophysical Research*, *114*(A3), A03207. https://doi.org/10.1029/2008JA013353

Tsyganenko, N. A. (1989). A magnetospheric magnetic field model with a warped tail current sheet. *Planetary and Space Science*, *37*(1), 5–20. https://doi.org/10.1016/0032-0633(89)90066-4

Usanova, M. E., Drozdov, A., Orlova, K., Mann, I. R., Shprits, Y., Robertson, M. T., et al. (2014). Effect of EMIC waves on relativistic and ultra-relativistic electron populations: Ground-based and Van Allen Probes observations. *Geophysical Research Letters*, *41*(5), 1375–1381. https://doi.org/10.1002/2013GL059024

Vomvoridis, J. L., Crystal, T. L., & Denavit, J. (1982). Theory and computer simulations of magnetospheric very low frequency emissions. *Journal of Geophysical Research*, *87*(A3), 1473–1489. https://doi.org/10.1029/JA087iA03p01473

Vomvoridis, J. L., & Denavit, J. (1979). Test particle correlation by a whistler wave in a nonuniform magnetic field. *Physics of Fluids*, *22*(2), 367–377. https://doi.org/10.1063/1.862589

Wang, B., Su, Z., Zhang, Y., Shi, S., & Wang, G. (2016). Nonlinear Landau resonant scattering of near equatorially mirroring radiation belt electrons by oblique EMIC waves. *Geophysical Research Letters*, *43*(8), 3628–3636. https://doi.org/10.1002/2016GL068467

Wang, X., Briguglio, S., Di Troia, C., Falessi, M., Fogaccia, G., Fusco, V., et al. (2022). Analysis of the nonlinear dynamics of a chirping-frequency Alfvén mode in a tokamak equilibrium. *Physics of Plasmas*, *29*(3), 032512. https://doi.org/10.1063/5.0080785

Wang, Y., Li, Y., Liu, K., Song, W., Xiong, Y., & Yao, F. (2023). Statistical analysis of electromagnetic ion cyclotron rising-tone emissions based on deep learning. *Journal of Geophysical Research: Space Physics*, *128*(5), e2022JA031085. https://doi.org/10.1029/2022JA031085

White, R. B., Goldston, R. J., McGuire, K., Boozer, A. H., Monticello, D. A., & Park, W. (1983). Theory of mode-induced beam particle loss in tokamaks. *Physics of Fluids*, *26*(10), 2958–2965. https://doi.org/10.1063/1.864060

Wu, Y., Tao, X., Zonca, F., & Chen, L. (2022). Nonlinear electron phase-space dynamics in spontaneous excitation of falling-tone chorus. *Geophysical Research Letters*, *49*(18), e2022GL100046. https://doi.org/10.1029/2022GL100046

Wu, Z., Huang, H., Wu, Y., Tao, X., Katoh, Y., & Wang, X. (2023). Connection between chorus wave amplitude and background magnetic field inhomogeneity: A parametric study. *Geophysical Research Letters*, *50*(24), e2023GL106397. https://doi.org/10.1029/2023GL106397

Xie, Y., Teng, S., Wu, Y., & Tao, X. (2021). A statistical analysis of duration and frequency chirping rate of falling tone chorus. *Geophysical Research Letters*, *48*(19), e2021GL095349. https://doi.org/10.1029/2021GL095349

Zhang, X.-J., Thorne, R., Artemyev, A., Mourenas, D., Angelopoulos, V., Bortnik, J., et al. (2018). Properties of intense field-aligned lower-band chorus waves: Implications for nonlinear wave-particle interactions. *Journal of Geophysical Research: Space Physics*, *123*(7), 5379–5393. https://doi.org/10.1029/2018JA025390

Zhou, Q., Xiao, F., Yang, C., He, Y., & Tang, L. (2013). Observation and modeling of magnetospheric cold electron heating by electromagnetic ion cyclotron waves. *Journal of Geophysical Research: Space Physics*, *118*(11), 6907–6914. https://doi.org/10.1029/2013JA019263

Zhu, H., Chen, L., Claudepierre, S. G., & Zheng, L. (2020). Direct evidence of the pitch angle scattering of relativistic electrons induced by EMIC waves. *Geophysical Research Letters*, *47*(4), e2019GL085637. https://doi.org/10.1029/2019GL085637

Zonca, F., Briguglio, S., Chen, L., Fogaccia, G., & Vlad, G. (2005). Transition from weak to strong energetic ion transport in burning plasmas. *Nuclear Fusion*, *45*(6), 477–484. https://doi.org/10.1088/0029-5515/45/6/009

Zonca, F., Tao, X., & Chen, L. (2021). Nonlinear dynamics and phase space transport by chorus emission. *Reviews of Modern Plasma Physics*, *5*(1), 1–44. https://doi.org/10.1007/s41614-021-00057-x

Zonca, F., Tao, X., & Chen, L. (2022). A theoretical framework of chorus wave excitation. *Journal of Geophysical Research: Space Physics*, *127*(2), e2021JA029760. https://doi.org/10.1029/2021JA029760